

Upregulation of the splice variant MUC4/Y in the pancreatic cancer cell line MIA PaCa-2 potentiates proliferation and suppresses apoptosis: New insight into the presence of the transcript variant of MUC4

KUNLING XIE^{1,2*}, XIAOFEI ZHI^{1,2*}, JIE TANG^{1,2*}, YI ZHU^{1,2}, JINGJING ZHANG^{1,2}, ZHENG LI^{1,2}, JINQIU TAO^{1,2} and ZEKUAN XU^{1,2}

¹Department of General Surgery, First Affiliated Hospital, Nanjing Medical University, Nanjing; ²Jiangsu Province Academy of Clinical Medicine, Institute of Tumor Biology, Nanjing, Jiangsu 210029, P.R. China

Received February 14, 2014; Accepted March 17, 2014

DOI: 10.3892/or.2014.3113

Abstract. MUC4/Y, the transcript variant 4 of MUC4, lacks exon 2 as compared with the transcript variant 1 of MUC4. To date, direct evidence for the function of MUC4/Y remains to be reported. Previous studies based their hypotheses regarding the function of MUC4/Y on the characteristic structure domains of this variant. The aim of the present study was to investigate the specific function of MUC4/Y. The pancreatic cancer cell line MIA PaCa-2 with low MUC4/Y expression was used to establish a stable cell model of MUC4/Y upregulation using a lentivirus vector system. Results showed that MUC4/Y anchored on the cytomembrane and affected cell morphology and cell cycle. Functional analyses indicated that MUC4/Y upregulation slightly potentiated cell proliferation and significantly suppressed apoptosis both *in vivo* and *in vitro*. Further studies revealed that the JNK and AKT signalling pathways were activated. Meanwhile, MUC4/Y upregulation elicited minimal effect on the phosphorylation level of HER2, a membrane partner of MUC4. These results suggest that MUC4/Y promotes tumour progression through its anti-apoptotic and weak mitogenic effect on MIA PaCa-2 cells.

Introduction

Mucins are high-molecular-weight, heavily O-glycosylated glycoproteins that serve as gel-forming components of

crude viscoelastic mucous gels for coating, lubricating and protecting the epithelial surfaces of the internal tracts of the body (1). Fourteen human mucin genes, namely, MUC1-4, MUC5B, MUC5AC, MUC6-8, MUC11-13, MUC16 and MUC17, have been identified thus far (2). All mucins share the similar structure that contains tandemly repeated amino acids. The membrane-associated mucin family member MUC4 has been reported in various types of cancer and inflammatory diseases, it has aberrant expression in pancreatic adenocarcinoma and pre-cancerous pancreatic intraepithelial neoplasias but minimal expression in normal pancreatic tissue and chronic pancreatitis (3). MUC4 predictably generates two functional subunits: MUC4 α (the mucin-like subunit) and MUC4 β (the transmembrane growth factor-like subunit). A similar feature can be observed in the homologous rat sialomucin complex (rat Muc4), which has been well characterised and investigated (4). MUC4 can produce at least 24 transcripts (sv0-MUC4 to sv21-MUC4, MUC4/X, MUC4/Y) (2). These splice transcripts can be expressed in three forms: membrane-bound, secreted and lacking the hallmark feature of mucin (MUC4/X and MUC4/Y). Splice variants of MUC4 are present in pancreatic carcinomas but not in normal pancreas (4). Thus, understanding the functions of these splice variants and the splicing process is necessary to determine their potential functions in pancreatic carcinomas. Different from sv0-MUC4, MUC4/Y lacks exon 2, which codes for the tandem repeat domain, however, MUC4/Y still contains the N-terminal and the transmembrane and cytoplasmic domains (4). Therefore, the functions of MUC4/Y need to be validated.

MUC4/Y is named by analogy with MUC1/Y. Compared with MUC1, MUC1/Y lacks tandemly repeated amino acids, as a well-established transcript form of MUC1, MUC1/Y has important functions in tumour initiation and progression (5-8). The aim of the present study was to determine the possible functions of MUC4/Y in tumour cell behaviour. The pancreatic cancer cell line MIA PaCa-2 with low MUC4/Y expression was used to construct a cell model of MUC4/Y upregulation.

Correspondence to: Dr Zekuan Xu, Department of General Surgery, First Affiliated Hospital, Nanjing Medical University, 300 Guangzhou Road, Nanjing, Jiangsu 210029, P.R. China
E-mail: 308050064@qq.com

*Contributed equally

Key words: MUC4/Y, MUC4, pancreatic cancer, proliferation, apoptosis

Materials and methods

Cell culture. The human pancreatic cancer cell lines MIA PaCa-2, PANC-1, BXPC-3, HPAC, COLO-357, CFPAC-1, T3M4 and PL-45 were purchased from the American Type Culture Collection. They were maintained in Dulbecco's modified Eagle's medium (DMEM) supplemented with 10% foetal bovine serum (FBS; Wisent, Canada) and antibiotics (1% penicillin/streptomycin; Gibco). All cell lines were grown in a humidified chamber supplemented with 5% CO₂ at 37°C.

Lentiviral production and infection. The MUC4/Y gene (NM_004532.4, 167736352) was synthesised artificially and cloned into the pUC57 plasmid (by Genscript Co., Nanjing, China). Lentiviral production was achieved using the pUC57 plasmid carrying MUC4/Y (by Shanghai SBO Medical Biotechnology Co.), with a three-plasmid system of pCDH-CMV-MCS-EF1-Puro, pCD/NL-BH*DDD and pLTR-G. The pancreatic cancer cell line MIA PaCa-2 was infected following the manufacturer's instructions. Stable cell lines were selected with 3 µg/ml of puromycin (Sigma, USA) for 4 days. The cells were analysed by real-time PCR and western blotting for MUC4/Y expression. The cells were then subjected to further assessments as follows.

RNA extraction and real-time RT-PCR. Total RNA was extracted from the cell lines with the TRIzol Reagent (Bio-Rad, USA). Extracted RNA was reverse transcribed into first-strand cDNA using IScript™ cDNA Synthesis Kit (Bio-Rad). The amount of cDNA used for the amplification of the target genes was normalised by the human GAPDH gene. The specific primers were: MUC4/Y forward, 5'-GTCCCAGGAATGACAACAC-3' and reverse, 5'-AATGGTGGAAATGATGTCTG-3'; GAPDH forward, 5'-ATCTCTGCCCCCTCTGCTGA-3' and reverse, 5'-GATGACCTTGCCACAGCCT-3'. Real-time PCR was performed on StepOnePlus Real-Time PCR System (Applied Biosystems, USA) using FastStart Universal SYBR-Green Master (Roche, Switzerland). All procedures were performed in triplicate. The 2^{-ΔΔCT} method (9) was used to calculate relative expression.

Protein extraction and western blot analysis. Total protein from cell lines was extracted using the protein extraction Kit (Key Gene, China). The protein extraction was loaded size-fractionated by sodium dodecyl sulphate-polyacrylamide gel electrophoresis and transferred to polyvinylidene fluoride membranes (Bio-Rad). The membranes were incubated overnight with specific primary antibodies in dilution buffer at 4°C. The antibodies against Bcl-2, Bcl-x1, Bax, CyclinD3, CDK-4, P27, Erk1/2, JNK, p38, c-Jun, AKT and HER2 were from Cell Signaling; GAPDH antibody was from Beyotime and 1G8 against MUC4/Y was from Invitrogen. The blotted membranes were incubated with horseradish peroxidase (HRP)-conjugated anti-mouse or rabbit IgG at room temperature for 2 h. The targeting protein expression level was detected using an enhanced chemiluminescence detection system. GAPDH was used as internal control.

Immunostaining of cell lines. The cells were fixed with Immunol Staining Fix Solution for 5 min (Beyotime, China),

pre-incubated with Immunol Staining Blocking Buffer (Beyotime) and then stained with monoclonal antibody against MUC4/Y. Nuclei were stained with 40-6-diamidino-2-phenylindole. Images were viewed and assessed under a fluorescence microscope.

Cell Counting Kit-8 (CCK-8) and plate colony formation assay. We used CCK-8 (Dojindo, Kumamoto, Japan) to detect cell proliferation. The cells were seeded into 96-well plates at a density of 2x10³/well. At the same time each day, 10 µl CCK-8 was added to each well. The absorbance at 450 nm was measured after the plate was incubated for 3 h in the incubator. For colony formation, two groups of stable cells (300 per well in six-well plates) were cultured in DMEM medium for 12 days. These colonies were photographed and statistically analysed.

Apoptosis assays. Alexa Fluor 647 Annexin V/7-ADD viability staining apoptosis detection Kit (Biolegend, San Diego, CA) was used to test cell apoptosis. Serum was deprived for 48 h before detection. Flow cytometry analysis was performed with a FACSCalibur flow cytometer (Gallios; Beckman Coulter, Brea, USA). The percentage of apoptosis was computed using Cell-Quest software (Becton Dickinson).

Cell cycle analysis. Synchronising cell cycle is important to cell cycle analysis. Thus, we first deprived serum for 24 h and then added serum back for 48 h incubation. Propidium iodide (Key Gene) was added into the tubes at a final concentration of 50 mg/l and then incubated in the dark for 30 min. The DNA content was analysed by a FACSCalibur flow cytometer (Gallios; Beckman Coulter). Data were processed using Wincycle32 software (Beckman Coulter).

In vivo tumourigenicity. Six nude mice (BALB/c nude mice, Vital River, Nanjing, China, four weeks old) were purchased to analyse tumour growth *in vivo*. MIA PaCa-2 cells that over-express MUC4/Y (MIA-MUC4/Y) and MIA PaCa-2 infected by empty vector (MIA-EV) cells were subcutaneously inoculated at a density of 1.5x10⁶ cells/animal into the flanks of nude mice. W and L were measured with calipers every 3 days, where W represents the smallest and L represents the largest diameter of the tumour. The mice were euthanised after 3 weeks. The volume of the implanted tumour was calculated using the formula: Volume = (W² x L)/2.

Immunohistochemistry (IHC) for subcutaneous graft. Max Vision™ techniques (Maixin Bio, China) were used for IHC according to the manufacturer's instructions. After blocking endogenous peroxides and proteins, 4 µm of slides were incubated overnight with diluted primary antibody against specific protein at 4°C. Then, the slices were incubated with HRP-polymer-conjugated secondary antibody at 37°C for 1 h. The slides were then stained by 3,3-diaminobenzidine solution for 3 min and then counterstained with haematoxylin.

In situ analyses of tumour apoptosis. The transplanted tumours were fixed in 4% formalin and then embedded in paraffin. A TUNEL apoptosis detection Kit (Key Gene, China) was used to detect cell apoptosis *in situ* according to the manufacturer's

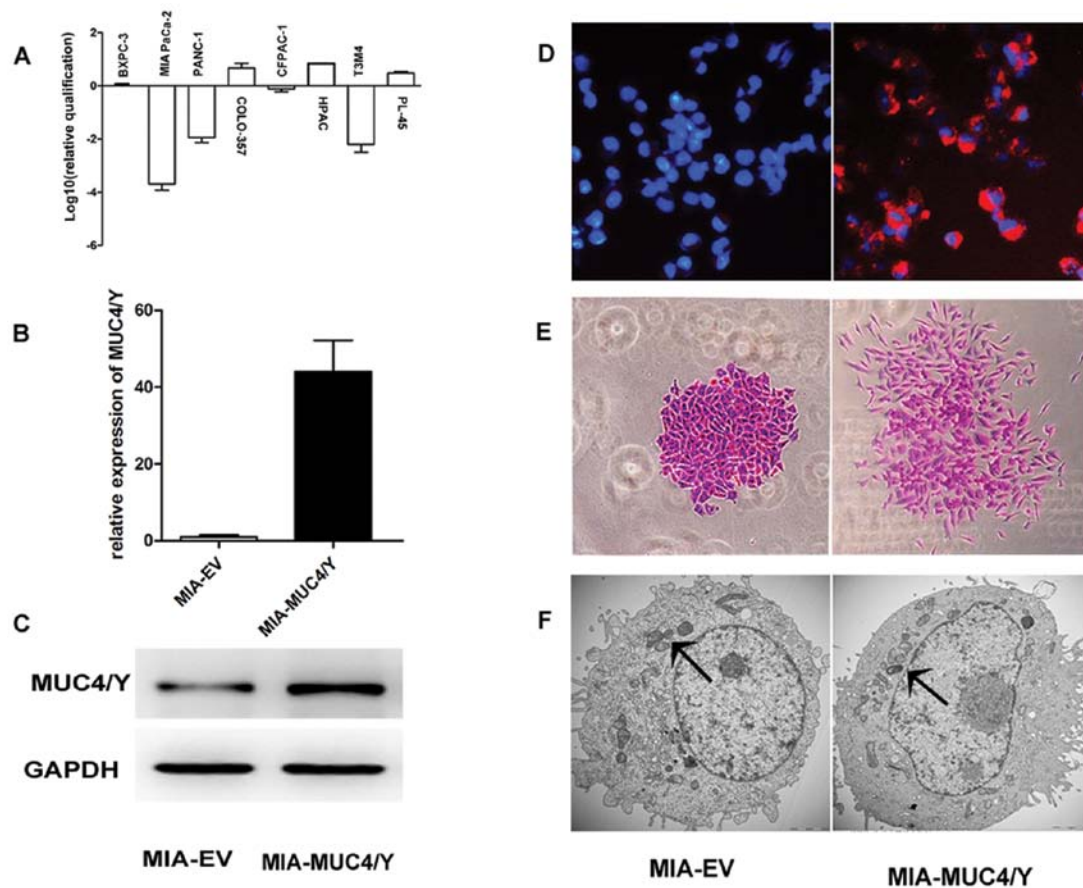


Figure 1. Expression of MUC4/Y in pancreatic adenocarcinoma cell lines, subcellular localisation of MUC4/Y and the effect of MUC4/Y on subcellular structure and cell morphology. (A) The mRNA level of MUC4/Y was tested with real-time PCR in eight pancreatic adenocarcinoma cell lines. The bar graphs represent gene expression levels relative to those in BXPC-3. HPAC, COLO-357 and PL45 cells showed high mRNA expression of MUC4/Y, whereas MIA PaCa-2, PANC-1, T3M4 and CFPAC-1 had low mRNA levels of MUC4/Y. (B and C) Real-time PCR and western blot analysis of MUC4/Y expression in MIA-EV and MIA-MUC4/Y cell lines. GAPDH was used as internal control. (D) Cell immunofluorescence located MUC4/Y in the cytoplasm and cytomembrane. (E) The colonies were photographed after they were stained by crystal violet. Cell shape was altered by MUC4/Y. (F) Electronic speculum showed that there were more mitochondria in MIA-MUC4/Y cells than in MIA-EV cells.

instruction. All slices were assessed under the microscope. The number of apoptotic cells was counted for quantitative analysis.

Statistical analysis. Data are expressed as the mean \pm standard deviation. Statistical analyses were performed using Statistical Package for Social Science 19. Differences of the mean between two groups were investigated by Student's t-test. $P < 0.05$ was considered to indicate a statistically significant difference. * $P < 0.05$, ** $P < 0.001$.

Results

Expression of MUC4/Y in pancreatic cancer cell lines, subcellular localisation of MUC4/Y in MIA PaCa-2 cells and effect of MUC4/Y on subcellular structure and cell morphology. The expression level of MUC4/Y was high in HPAC, COLO-357 and PL-45 but very low in MIA PaCa-2 and PANC-1 (Fig. 1A). The upregulation of MUC4/Y was affirmed by real-time PCR and western blotting (Fig. 1B and C). Cell immunofluorescence showed that MUC4/Y can anchor on the cytomembrane and cytoplasm (Fig. 1D). Formatted colony showed that MUC4/Y upregulation affected cell morphology. Compared

with MIA-EV cells, MIA-MUC4/Y cells lost highly aggregated architecture and cell-cell interaction, and became slightly elongated (Fig. 1E). Electronic speculum indicated that MUC4/Y increased the number of mitochondria (Fig. 1F).

Effect of MUC4/Y on tumour growth. We studied the effect of MUC4/Y on tumourigenicity *in vivo*. MIA-MUC4/Y cells were injected into a flank of nude mice to form ectopic tumours, and MIA-EV cells were inoculated into the opposite flank of the same mice. Comparison of the tumour size of the MIA-MUC4/Y group with that of the MIA-EV group showed that MUC4/Y significantly promoted tumourigenicity (* $P < 0.05$; Fig. 2A and E). Many factors affect tumour expansion, these factors include secretion of metalloproteinase, tumour neovascularisation, proliferation and apoptosis caused by environmental stress. The possible function of MUC4/Y involved in anti-apoptosis was tested by TUNEL staining *in situ*. The results showed that MUC4/Y markedly suppressed apoptosis compared with MIA-EV (* $P < 0.05$; Fig. 2B and F). The results of IHC for subcutaneous graft targeting Ki-67 indicated that the MIA-MUC4/Y group had a more powerful proliferation state than the MIA-EV group (* $P < 0.05$; Fig. 2C and G). The expression of HER2 did not significantly

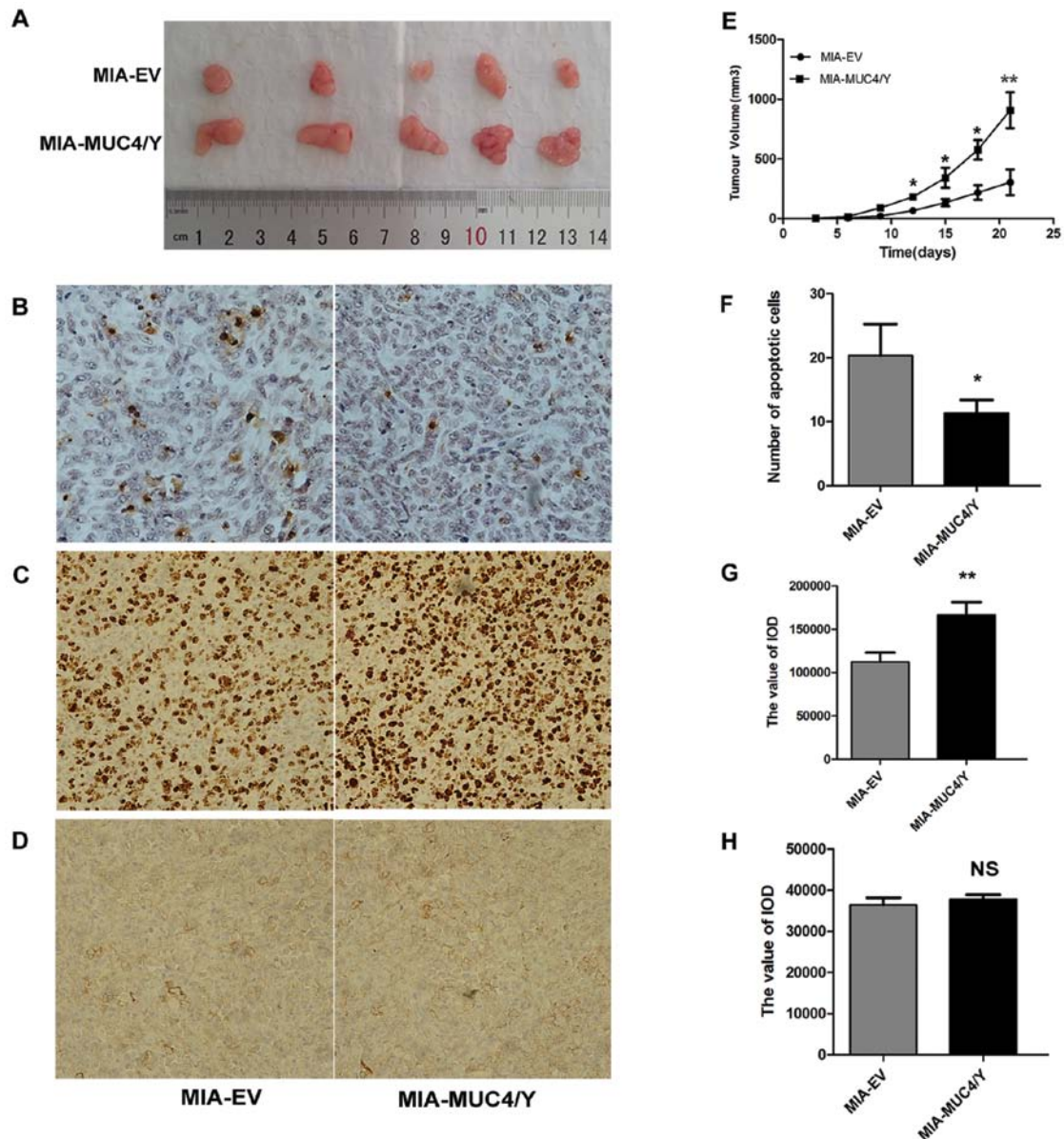


Figure 2. Effect of MUC4/Y on tumour growth. (A and E) MUC4/Y upregulation accelerated tumour growth compared with the MIA-EV group. (B and F) The effect of MUC4/Y on apoptosis in implanted tumours of the MIA-MUC4/Y and MIA-EV groups were determined by TUNEL assay. The number of apoptotic cells was counted and compared. The result is presented in a histogram ($P < 0.05$). (C and G) Effect of MUC4/Y on proliferation in the above implanted tumours was studied by immunohistochemical assay against Ki-67. Histograms of their integrated optical density (IOD) value were measured ($**P < 0.001$). (D and H) The expression level of HER2 in both MIA-MUC4/Y and MIA-EV groups was determined by immunohistochemical assay against HER2. Histograms of their integrated optical density (IOD) value were measured. NS, not significant.

change (Fig. 2D and H). These data suggest that MUC4/Y contributes to tumour growth.

Effect of MUC4/Y on cell cycle and proliferation *in vitro*. We employed the CCK-8 assay to evaluate the intrinsic effects of MUC4/Y on cell growth *in vitro*. As shown in Fig. 3C, the growth histograms according to absorbance indicated that MUC4/Y slightly increased the optical density compared with MIA-EV. Plate colony formation assay was employed to evaluate the long effects of MUC4/Y on cell proliferation. As shown in Fig. 3A, the number of formatted colony in the MIA-MUC4/Y group was close to that of the MIA-EV group, but the colony size of the MIA-MUC4/Y group was significantly larger than that of the MIA-EV group. The cell cycle

was tested to further explain the difference in proliferation. As shown in Fig. 3B and E, the S phase had higher percentage in the MIA-MUC4/Y group than in the MIA-EV group. CyclinD3, CDK4 and P27 are associated with G0/G1 transition (10,11). Western blot analysis showed that P27 expression was markedly reduced. CDK-4 expression was increased. Of note, CyclinD3 expression was slightly downregulated (Fig. 3F), which may account for considerable downregulation in P27 contributed to the weak mitogenic effect of MUC4/Y. These data demonstrated that MUC4/Y promoted cell proliferation *in vitro*. This observation is consistent with that *in vivo*.

Suppression of cell apoptosis by MUC4/Y *in vitro*. MUC4/Y suppressed MIA PaCa-2 cell apoptosis *in vivo*. The different

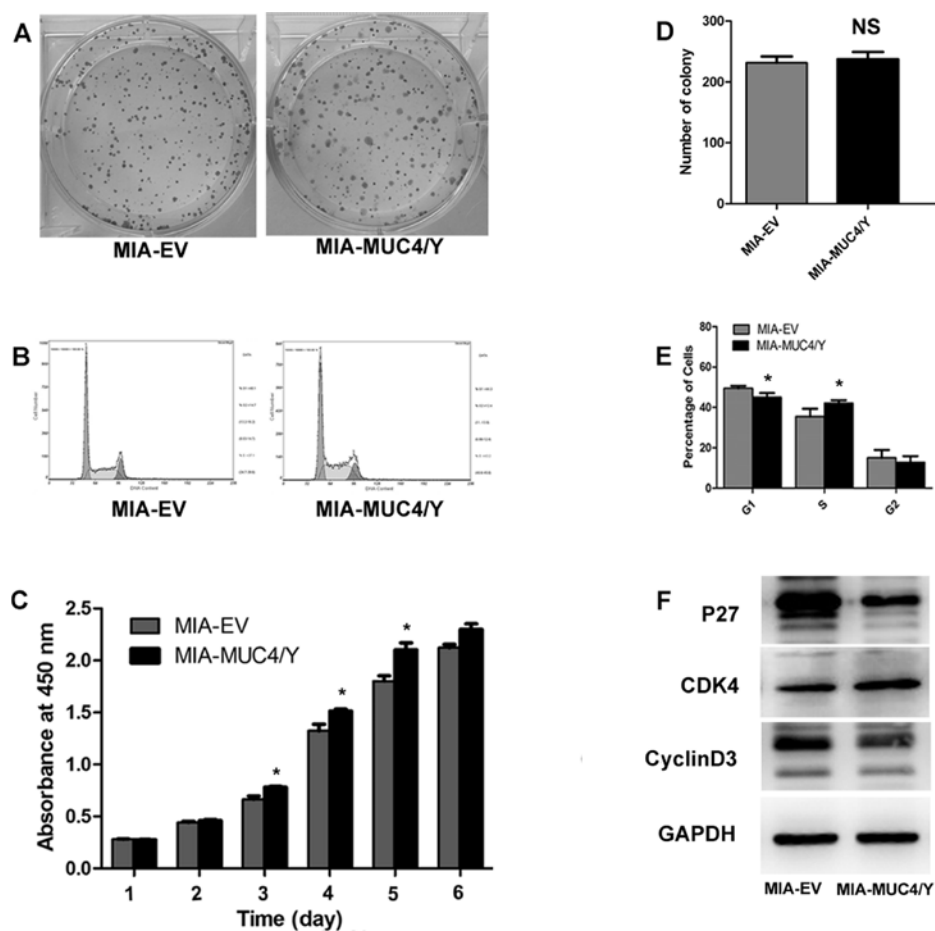


Figure 3. Effect of MUC4/Y on cell proliferation *in vitro*. (A and D) The colonies number in the MIA-MUC4/Y group was close to that in the MIA-EV group, whereas the colony size in the MIA-MUC4/Y group was larger than that in the MIA-EV group. The result is also presented in a histogram. (B and E) Cell cycle test indicated that MUC4/Y can alleviate G1 arrest; more cells in the S phase were detected in the MUC4/Y group than in the MIA-EV group (*P<0.05). (C) The absorbance at 450 nm was measured 3 h later after CCK-8 was added. Results indicated that the proliferation ability of MIA-MUC4/Y was stronger than that of MIA-EV (*P<0.05). (F) Western blot analysis demonstrated that P27 was downregulated and that CDK4 was upregulated in MUC4/Y cells; however, the expression level of CyclinD3 was downregulated. GAPDH was used as the internal control.

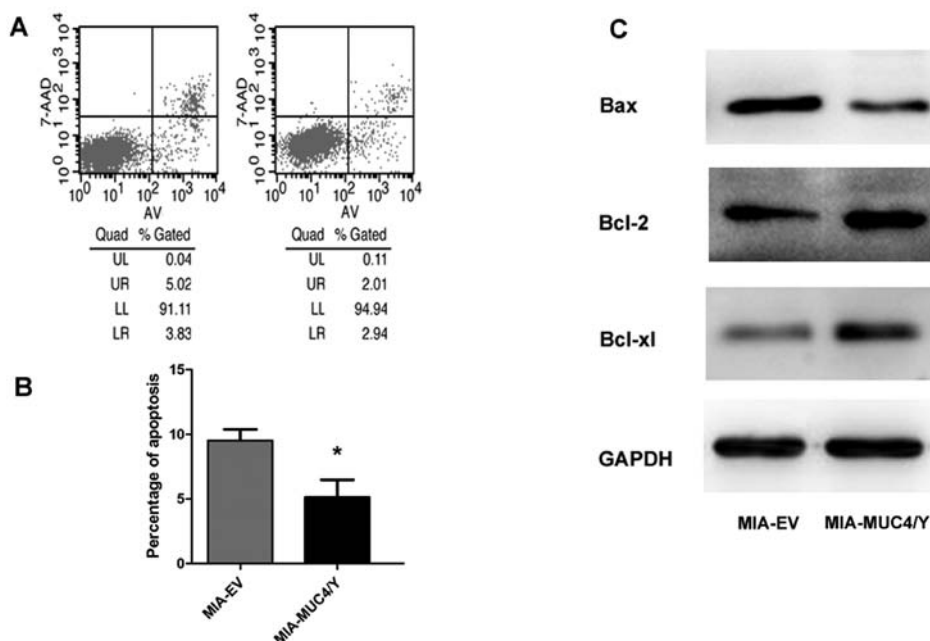


Figure 4. Effect of MUC4/Y on apoptosis *in vitro*. (A and B) Flow cytometry analysis was conducted to determine apoptosis. MUC4/Y suppressed apoptosis (*P<0.05). (C) Western blot analysis indicated that Bcl-2 and Bcl-xl were increased and that Bax was decreased in the MIA-MUC4/Y group compared with the MIA-EV group. GAPDH was used as internal control.

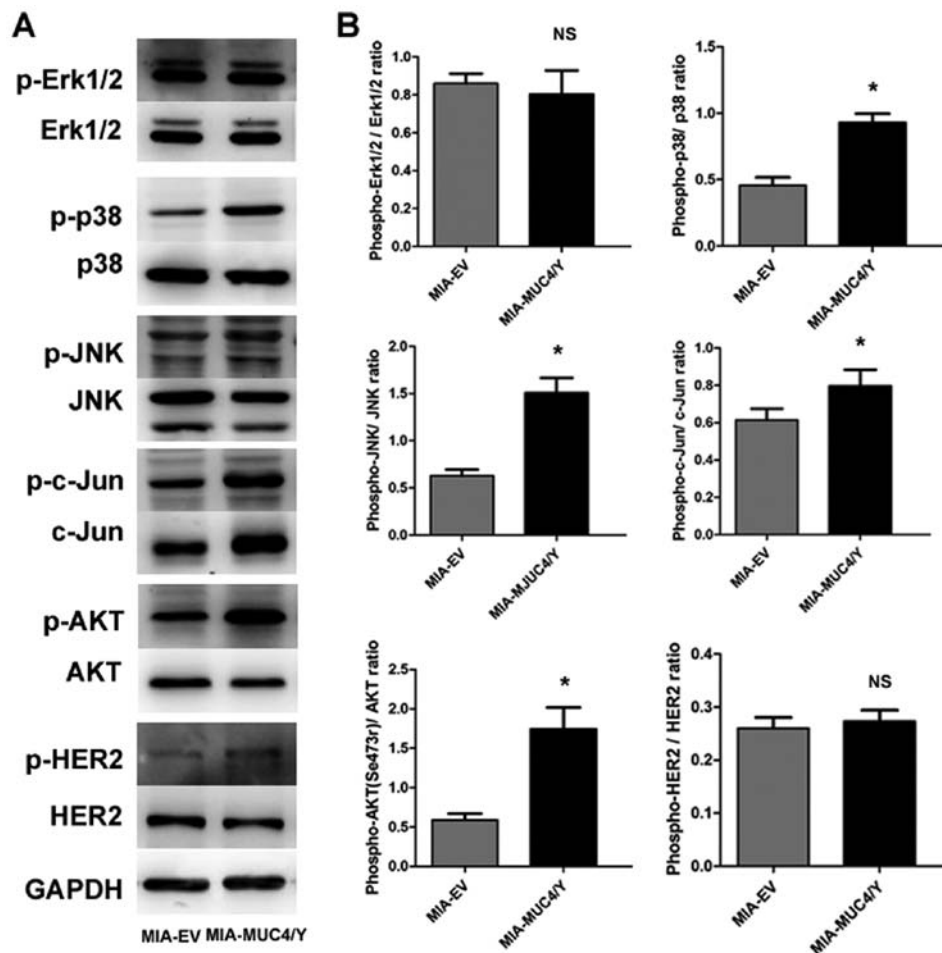


Figure 5. Effect of MUC4/Y on MAPK (Erk1/2, JNK, P38), c-Jun and AKT signalling pathways. (A) Western blot analysis was performed to determine both phosphorylated and constitutive forms of Erk1/2, JNK, p38, c-Jun, AKT and HER2. GAPDH was used as the internal control. (B) Bands were quantified by densitometry. Histograms of the ratio (phosphorylated/constitutive form) for Erk1/2, JNK, p38, c-Jun, AKT and HER2 are presented ($P < 0.05$). NS, not significant. The phosphorylation levels of JNK, p38, c-Jun and AKT were increased. The expression and phosphorylation of Erk1/2 were not altered. The phosphorylation level of HER2 was not significantly altered by MUC4/Y.

functions of MIA-MUC4/Y and MIA-EV in tumour neovascularisation as well as the increased secretion of matrix metalloproteinase due to MUC4/Y can alter tumour-stroma interaction, which in turn affect apoptosis (12). We analysed the apoptosis levels of MIA-MUC4/Y and MIA-EV *in vitro* to investigate the anti-apoptotic function of MUC4/Y independent of tumour-stroma interaction. As shown in Fig. 4A ($P < 0.05$), the apoptosis level of the MUC4/Y group decreased compared with that of the MIA-EV group. Furthermore, western blot analysis showed that the expression levels of anti-apoptosis proteins Bcl-2 and Bcl-x1 increased in MIA-MUC4/Y cells (Fig. 4C). Correspondingly, the expression level of Bax in MIA-MUC4/Y cells was downregulated compared with that in MIA-EV cells. These results indicated that the mitochondrial pathways (intrinsic pathway) were involved in the anti-apoptotic function of MUC4/Y.

Effect of MUC4/Y on signalling pathways. Cells displaying uncontrolled proliferation due to constitutive activation of growth factor signalling contribute to malignant transformation (13). PI3-kinase, which is commonly activated by growth factor receptors, activates the serine/threonine kinase AKT to mediate a series of phosphorylation events that promote cellular

survival (14). p38, c-Jun and Erk1/2, which belong to mitogen-activated protein kinases, are also important targets of growth factor signalling that elicit diverse cellular responses, including cellular survival (15). In the present study, we detected the phosphorylated and constitutive form levels of Erk1/2, JNK, P38, c-Jun, AKT and HER2. As shown in Fig. 5B ($P < 0.05$), the ratio (phosphorylated/constitutive form) of HER2 was not significantly altered and Erk1/2 was not changed. Meanwhile, the phosphorylated/constitutive form ratios of JNK, c-Jun, P38 and AKT significantly increased in the MIA-MUC4/Y groups compared with those in the MIA-EV group.

Discussion

MUC4/Y is generated by deleting exon 2, which corresponds to exon skipping by the alternative use of acceptor sites. The alternative use of exon as the most common mechanism to generate isoforms is involved in MUC4 transcripts, the same mechanism is present in several MUC4 transcripts, suggesting that MUC4/Y is not generated due to a splicing error (2). The alternative mRNA splice forms may only function to downregulate the expression of the main functional form sv0-MUC4 (2). In the present study, MUC4/Y in the cytomembrane could

affect cell function in proliferation and apoptosis both *in vivo* and *in vitro*. MUC4/Y retains some characteristic domains of MUC4, and some splicing variants of MUC4 encode the same protein. Thus, we deduced that different splicing variants of MUC4 may have certain functions (similar to MUC1) and that different proportions of MUC4 splicing variants may modulate the properties of MUC4. Previous studies revealed that rat Muc4 O-glycosylation domain is dispensable for its anti-apoptotic activity (16) and that the O-glycosylation domain of mucin Mbs2 suppresses signalling through the HOG1 MAPK pathway (17). Those studies suggest that splicing variants that lack the O-glycosylation domain can still promote tumour progression. The O-glycosylation domain is necessary for the efficient disruption of cell-cell and cell-substrate interactions (16,18). Thus, the presence of this domain could facilitate early events in tumour initiation (19) but may be dispensable at later stages of tumour development. Different transcript variants of MUC4 are comprised of different structural domains. The multiple functions of MUC4, which are attributed to its multiple characteristic structure domains, may also be a result of its diversity variants in different periods of tumour progression.

The MUC4/HER2 (ErbB2) complex has been observed (20-22) both in MUC4 normally- and aberrantly-expressed tissues. MUC4 and HER2 are frequently overexpressed in pancreatic cancer and in PanINs (22). To date, there is no known ligand for HER2 (23), but HER2 can act as a membrane partner of MUC4. MUC4 enhances cellular proliferation by interacting with HER2 (22). In CAPAN-2 cells, HER2 is downregulated when MUC4 is knocked down, and MUC4 is downregulated when HER2 is knocked down. However, the effects of MUC4 or HER2-knockdown on signalling pathways vary, namely, MUC4 knockdown affects the JNK pathway, whereas HER2-knockdown alters the MAPK pathway (22). In the present study, the upregulation of MUC4/Y in MIA PaCa-2 cells did not obviously alter the expression level of HER2, and the phosphorylation level of HER2 was activated in a limited manner. Previous studies indicated that the HER2-mediated activation of the Erk1/2 pathway is crucial in mediating cancer cell growth and proliferation (22-24). Correspondingly, Erk1/2 was also not affected by MUC4/Y upregulation in the present study. Previous studies revealed that rat Muc4, as the intramembrane HER2 ligand, induces limited phosphorylation of HER2 and does not activate the Erk1/2 pathway without the neuregulin-mediated activation of HER3 and HER2. In this context, upregulation of the cell-cycle inhibitor P27 has been associated with anti-apoptosis (25). In the present study, P27 was markedly downregulated. These data suggest that limited phosphorylation of HER2 may also be involved in the function of MUC4/Y. Otherwise, the presence of new unidentified partners of MUC4/Y for signal transduction is strongly suggested as the cytoplasmic domain of MUC4/Y is too short to transduce and activate downstream signals.

The paradoxical regulation of P27 indicates that other signalling pathways regulated by MUC4/Y are involved in its anti-apoptotic function. Previous studies revealed that AKT is involved in cell cycle regulation by negatively regulating P27 (26). This result is consistent with the present findings. In addition, growth factor-induced activation of AKT via P38 is a pro-survival pathway in lung cells (27). The transcriptional

activity of c-Jun is regulated by phosphorylation at Ser63 and Ser73 through SAPK/JNK-activated JNK, and the downstream target AP-1 is involved in proliferation and apoptosis (28). The previously identified function of the JNK pathway in apoptotic regulation through Bcl-2/Bcl-XL phosphorylation (29) is consistent with our results. These data indicate that multiple signalling pathways are affected by MUC4/Y. Thus, MUC4/Y may have more functions in tumour progression.

The present study is the first to demonstrate the functions of MUC4/Y in anti-apoptosis and pro-proliferation. This study also showed that multiple signalling pathways were affected by MUC4/Y. MUC4/Y can anchor itself on the cytomembrane, suggesting that it can be classified into the membrane-bound forms. MUC4 is difficult to investigate due to its high molecular weight. The function of MUC4/Y identified in the present study could be used as basis for directly investigating the other structural domains (AMOP, NIDO and vWD) of MUC4.

Acknowledgements

This study was partially supported by the National Natural Science Foundation of China (81272712, 81072031, 81101802), the Natural Science Foundation of Jiangsu Province (BK2010585, BK2011845), the Program for Development of Innovative Research Team in the First Affiliated Hospital of NJMU, the Priority Academic Program Development of Jiangsu Higher Education Institutions (PAPD, JX10231801), and the translational research of early diagnosis and comprehensive treatment in pancreatic cancer (the Research Special Fund for the Public Welfare Industry of Health, 201202007).

References

1. Mall AS: Analysis of mucins: role in laboratory diagnosis. *J Clin Pathol* 61: 1018-1024, 2008.
2. Escande F, Lemaitre L, Moniaux N, Batra SK, Aubert JP and Buisine MP: Genomic organization of MUC4 mucin gene. Towards the characterization of splice variants. *Eur J Biochem* 269: 3637-3644, 2002.
3. Andrianifahanana M, Moniaux N, Schmied BM, *et al*: Mucin (MUC) gene expression in human pancreatic adenocarcinoma and chronic pancreatitis: a potential role of MUC4 as a tumor marker of diagnostic significance. *Clin Cancer Res* 7: 4033-4040, 2001.
4. Chaturvedi P, Singh AP and Batra SK: Structure, evolution, and biology of the MUC4 mucin. *FASEB J* 22: 966-981, 2008.
5. Moniaux N, Escande F, Batra SK, Porchet N, Laine A and Aubert JP: Alternative splicing generates a family of putative secreted and membrane-associated MUC4 mucins. *Eur J Biochem* 267: 4536-4544, 2000.
6. Baruch A, Hartmann M, Zrihan-Licht S, *et al*: Preferential expression of novel MUC1 tumor antigen isoforms in human epithelial tumors and their tumor-potentiating function. *Int J Cancer* 71: 741-749, 1997.
7. Baruch A, Hartmann M, Yoeli M, *et al*: The breast cancer-associated MUC1 gene generates both a receptor and its cognate binding protein. *Cancer Res* 59: 1552-1561, 1999.
8. Zrihan-Licht S, Baruch A, Elroy-Stein O, Keydar I and Wreschner DH: Tyrosine phosphorylation of the MUC1 breast cancer membrane proteins. Cytokine receptor-like molecules. *FEBS Lett* 356: 130-136, 1994.
9. Livak KJ and Schmittgen TD: Analysis of relative gene expression data using real-time quantitative PCR and the 2(-Delta Delta C(T)) Method. *Methods* 25: 402-408, 2001.
10. Sherr CJ: Cancer cell cycles. *Science* 274: 1672-1677, 1996.
11. Lukas J, Bartkova J and Bartek J: Convergence of mitogenic signalling cascades from diverse classes of receptors at the cyclin D-cyclin-dependent kinase-pRb-controlled G1 checkpoint. *Mol Cell Biol* 16: 6917-6925, 1996.

12. Komatsu M, Jepson S, Arango ME, Carothers Carraway CA and Carraway KL: Muc4/sialomucin complex, an intramembrane modulator of ErbB2/HER2/Neu, potentiates primary tumor growth and suppresses apoptosis in a xenotransplanted tumor. *Oncogene* 20: 461-470, 2001.
13. Croce CM: Oncogenes and cancer. *N Engl J Med* 358: 502-511, 2008.
14. Cantley LC: The phosphoinositide 3-kinase pathway. *Science* 296: 1655-1657, 2002.
15. Junttila MR, Li SP and Westermarck J: Phosphatase-mediated crosstalk between MAPK signaling pathways in the regulation of cell survival. *FASEB J* 22: 954-965, 2008.
16. Workman HC, Sweeney C and Carraway KL III: The membrane mucin Muc4 inhibits apoptosis induced by multiple insults via ErbB2-dependent and ErbB2-independent mechanisms. *Cancer Res* 69: 2845-2852, 2009.
17. Cullen PJ, Sabbagh W Jr., Graham E, *et al*: A signaling mucin at the head of the Cdc42- and MAPK-dependent filamentous growth pathway in yeast. *Genes Dev* 18: 1695-1708, 2004.
18. Komatsu M, Carraway CA, Fregien NL and Carraway KL: Reversible disruption of cell-matrix and cell-cell interactions by overexpression of sialomucin complex. *J Biol Chem* 272: 33245-33254, 1997.
19. Carraway KL, Ramsauer VP and Carraway CA: Glycoprotein contributions to mammary gland and mammary tumor structure and function: roles of adherens junctions, ErbBs and membrane MUCs. *J Cell Biochem* 96: 914-926, 2005.
20. Ramsauer VP, Pino V, Farooq A, Carothers Carraway CA, Salas PJ and Carraway KL: Muc4-ErbB2 complex formation and signaling in polarized CACO-2 epithelial cells indicate that Muc4 acts as an unorthodox ligand for ErbB2. *Mol Biol Cell* 17: 2931-2941, 2006.
21. Chaturvedi P, Singh AP, Chakraborty S, *et al*: MUC4 mucin interacts with and stabilizes the HER2 oncoprotein in human pancreatic cancer cells. *Cancer Res* 68: 2065-2070, 2008.
22. Jonckheere N, Skrypek N, Merlin J, *et al*: The mucin MUC4 and its membrane partner ErbB2 regulate biological properties of human CAPAN-2 pancreatic cancer cells via different signalling pathways. *PLoS One* 7: e32232, 2012.
23. Moasser MM: The oncogene HER2: its signaling and transforming functions and its role in human cancer pathogenesis. *Oncogene* 26: 6469-6487, 2007.
24. Bafna S, Kaur S and Batra SK: Membrane-bound mucins: the mechanistic basis for alterations in the growth and survival of cancer cells. *Oncogene* 29: 2893-2904, 2010.
25. Jepson S, Komatsu M, Haq B, *et al*: Muc4/sialomucin complex, the intramembrane ErbB2 ligand, induces specific phosphorylation of ErbB2 and enhances expression of p27(kip), but does not activate mitogen-activated kinase or protein kinaseB/Akt pathways. *Oncogene* 21: 7524-7532, 2002.
26. Gesbert F, Sellers WR, Signoretti S, Loda M and Griffin JD: BCR/ABL regulates expression of the cyclin-dependent kinase inhibitor p27Kip1 through the phosphatidylinositol 3-Kinase/AKT pathway. *J Biol Chem* 275: 39223-39230, 2000.
27. Horowitz JC, Lee DY, Waghray M, *et al*: Activation of the pro-survival phosphatidylinositol 3-kinase/AKT pathway by transforming growth factor-beta1 in mesenchymal cells is mediated by p38 MAPK-dependent induction of an autocrine growth factor. *J Biol Chem* 279: 1359-1367, 2004.
28. Davis RJ: Signal transduction by the JNK group of MAP kinases. *Cell* 103: 239-252, 2000.
29. Fan M, Goodwin M, Vu T, Brantley-Finley C, Gaarde WA and Chambers TC: Vinblastine-induced phosphorylation of Bcl-2 and Bcl-XL is mediated by JNK and occurs in parallel with inactivation of the Raf-1/MEK/ERK cascade. *J Biol Chem* 275: 29980-29985, 2000.